JBC RESEARCH ARTICLE

BANCR-containing extracellular vesicles enhance breast cancer resistance

Received for publication, July 26, 2024, and in revised form, December 11, 2024 Published, Papers in Press, February 11, 2025,
https://doi.org/10.1016/j.jbc.2025.108304

Xinming Song, Shen Liu, Ying Zeng, Yilin Cai, and Haiqing Luo*

From the Department of Head and Neck Oncology, Affiliated Hospital of Guangdong Medical University, Zhanjiang, China

Reviewed by members of the JBC Editorial Board. Edited by Paul Shapiro

Extracellular vesicles (EVs) are nano-sized particles secreted by many cell types—including tumor cells—and play key roles in cellular communication by transporting functional RNAs. This study aims to elucidate the role of long noncoding RNA BRAF-activated nonprotein coding RNA (BANCR) in EVs derived from breast cancer (BC) cells in trastuzumab resistance. Differentially expressed long noncoding RNA and downstream targets in BC-resistant samples were identified. SKBR-3 cells were treated with trastuzumab to generate resistant cells (SKBR-3TR), and EVs from these cells (SKBR-3TR-EVs) were isolated and characterized. Functional studies of BANCR were performed in SKBR-3 and SKBR-3TR cells. Coculturing SKBR-3 cells with SKBR-3TR-EVs assessed changes in cell behavior. A xenograft model in nude mice examined *in vivo* tumorigenicity and trastuzumab resistance. BANCR was highly expressed in SKBR-3TR cells and EVs, linked to trastuzumab resistance. SKBR-3TR-EVs transferred BANCR to SKBR-3 cells, where BANCR inhibited miR-34a-5p, reducing its expression. High-mobility group A1 (HMGA1) was identified as a miR-34a-5p target. BANCR activated the HMGA1/Wnt/β-catenin pathway by inhibiting miR-34a-5p, promoting resistance. *In vivo* experiments showed that BANCR inhibition delayed tumorigenesis and reversed trastuzumab resistance. BC cell–derived EVs containing BANCR may enhance resistance to trastuzumab by regulating the miR-34a-5p/HMGA1/Wnt/β-catenin axis, presenting a potential target for BC therapy.

Breast cancer (BC) is a prevalent malignancy in women and is a major cause of cancer-related deaths in the female population (1). Trastuzumab is a recombinant antibody targeting HER2 and remains the standard of care for the early and advanced stages of HER2-positive BC (2). However, a subpopulation of patients exhibits resistance to trastuzumab, which challenges the use of this drug in improving the clinical outcome of patients (3, 4). Investigation into the mechanism of trastuzumab resistance and the innovative therapies are thus required.

Tumor-derived extracellular vesicles (EVs) can regulate the resistance of tumor cells to anticancer drugs by carrying a variety of biomolecules, including long noncoding RNAs (lncRNAs) (5, 6). BRAF-activated nonprotein coding RNA (BANCR), located in a gene desert region on 9q21.11-q21.12, has been implicated in tumorigenesis by affecting cellular functions, including proliferation, migration, invasion, and apoptosis (7). BANCR is highly expressed in BC, and this high expression can promote the growth, invasion, and metastasis of BC cells (8). BANCR silencing can potentiate the sensitivity of colorectal cancer cells to adriamycin (9). However, its role in the drug resistance of BC remains elusive.

BANCR binds to the sequence of miR-34a-5p, predicted by the RNA22 website (https://cm.jefferson.edu/rna22/Interactive/). miR-34 has been identified as a promising target for RNA-based therapy in invasive BC (10). Overexpression of miR-34 potently suppresses the proliferation of BC, induces cell apoptosis *in vitro* and reduces the tumorigenicity of BC *in vivo* (11). Transfection with miR-34a mimic in MDR-MCF-7 BC cells leads to a partial reversal of multidrug resistance (12). StarBase (https://starbase.sysu.edu.cn/) and miRWalk (http://mirwalk.umm.uni-heidelberg.de/) websites predicted the presence of miR-34a-5p binding sites in the 3′UTR of high-mobility group A1 (HMGA1) mRNA. HMGA1, a chromatin remodeling factor abundantly expressed in many different cancers (13), can exacerbate the drug resistance of cancer cells *in vitro* (PMID: 33536786; 31814893). Additionally, HMGA1 can positively regulate the Wnt/β-catenin pathway by interacting with β-catenin (14, 15). Notably, activation of the Wnt/β-catenin pathway enhances the chemoresistance of BC cells (16).

Hence, we hypothesized that BANCR might regulate the trastuzumab resistance in BC, associated with the miR-34a-5p/HMGA1/Wnt/β-catenin axis. Herein, the expression and biological role of BANCR in BC trastuzumab-resistant cells were explored. In addition, the relationship among BANCR, miR-34a-5p, and HMGA1 was also studied in the current research.

Results

Bioinformatics analysis predicts the effect of EVs on the resistance of BC cells to trastuzumab via *BANCR transfer*

Analysis of the lncRNA expression dataset GSE155478 revealed 1103 significantly upregulated and 1849 significantly downregulated lncRNAs in the BC-resistant samples (Fig. 1, *A* and *B*). The analysis results of the GSE115040 dataset showed

* For correspondence: Haiqing Luo, linjing@fahostumc.com.

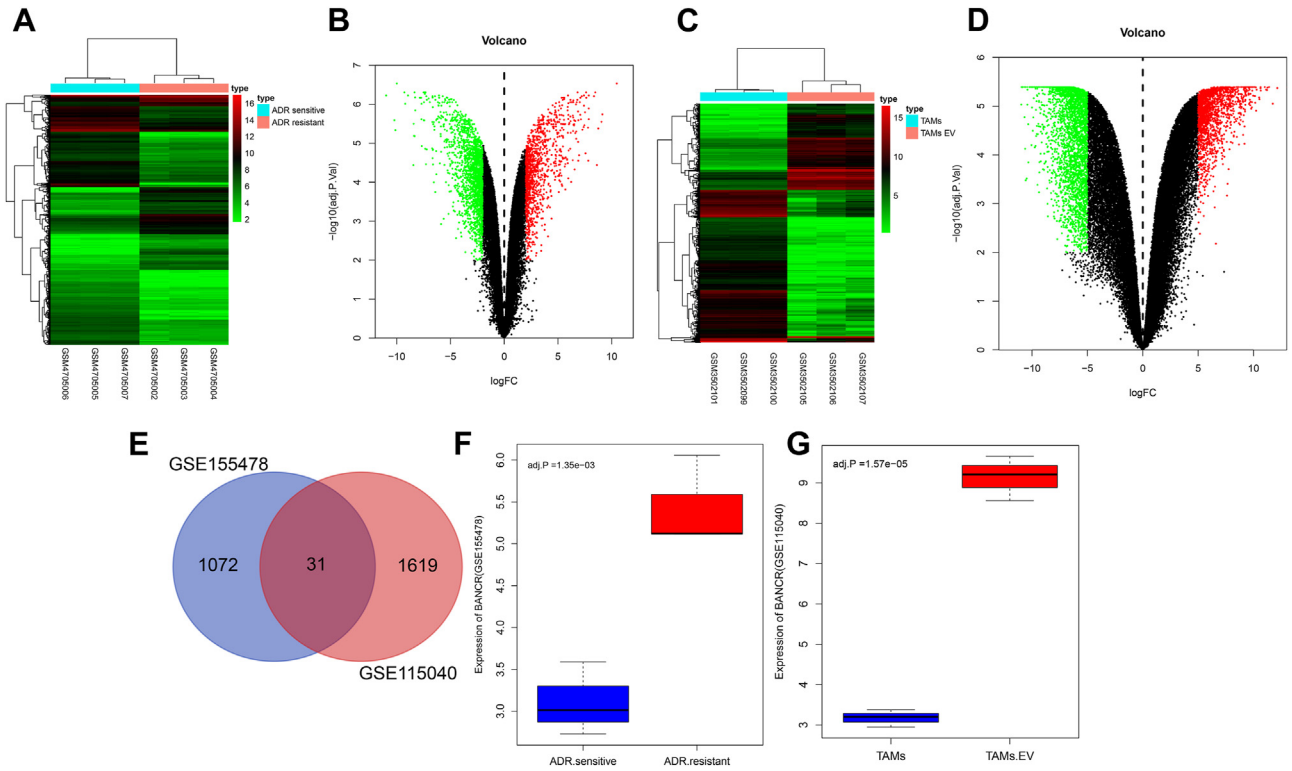

Figure 1. Significance of lncRNAs in the resistance of BC cells to trastuzumab. *A,* a heat map showing the differentially expressed lncRNAs in trastuzumab-resistant (n = 3) and trastuzumab-sensitive cell line samples (n = 3) in the GSE155478 dataset. *B,* a volcano map showing the differentially expressed lncRNAs in trastuzumab-resistant (n = 3) and trastuzumab-sensitive cell line samples (n = 3) in the GSE155478 dataset. *Red* indicates up-regulated lncRNAs, and *green* indicates downregulated lncRNAs. *C,* a heat map showing the differentially expressed lncRNAs in EVs (n = 3) and BC cells (n = 3) in the GSE115040 dataset. *D,* a volcano map showing the differentially expressed lncRNAs in EVs (n = 3) and BC cells (n = 3) in the GSE115040 dataset. *Red* indicates upregulated lncRNAs, and *green* indicates downregulated lncRNAs. *E,* Venn diagram of the upregulated lncRNAs from the GSE155478 and GSE155478 datasets. The *blue circle* represents the highly expressed lncRNAs in drug-resistant BC cells in the GSE155478 dataset, while the *red circle* indicates the highly expressed lncRNAs in EVs in the GSE115040 dataset. *F,* BANCR expression in trastuzumab-resistant (n = 3) and trastuzumab-sensitive cell line samples (n = 3) in the GSE155478 dataset. *G,* BANCR expression in EVs (n = 3) and BC cells (n = 3) in the GSE115040 dataset. LncRNA, long noncoding RNA; EV, extracellular vesicle; BANCR, BRAF-activated nonprotein coding RNA; BC, breast cancer.

1650 markedly upregulated lncRNAs and 2788 markedly downregulated lncRNAs in EVs (Fig. 1, *C* and *D*). Following the Venn diagram of the significantly upregulated lncRNAs in the BC-resistant samples and in EVs, 31 lncRNAs were found at the intersection, such as BANCR, SNORD123, CGA, SMTNL2, LRTM1, and ARHGEF26 (Fig. 1*E*).

In addition, GSE155478 dataset analysis results demonstrated remarkably higher BANCR expression in BC-resistant cell line samples than in BC-sensitive cell line samples (Fig. 1*F*). Meanwhile, the analysis data of the GSE115040 dataset showed that the BANCR expression was significantly higher in EVs than in BC cells (Fig. 1*G*).

Collectively, we speculate that EVs may affect the resistance of BC cells to trastuzumab by mediating the transfer of BANCR.

Overexpression of BANCR promotes resistance of BC cells to trastuzumab

Next, we moved to clarify the relationship between BANCR and trastuzumab resistance in BC cells. quantitative real-time polymerase chain reaction (qRT-PCR) data showed higher BANCR expression in SKBR-3TR than SKBR-3 cells (Fig. 2*A*).

In addition, SKBR-3TR were transduced with lentivirus harboring sh-BANCR and SKBR-3 cells were transduced with lentivirus harboring overexpression of BANCR (oe-BANCR). qRT-PCR verified the successful transduction (Fig. 2*B*). Subsequent CCK-8 results revealed the IC_{50} value of trastuzumab was decreased after BANCR downregulation in SKBR-3TR, while opposite results were found upon oe-BANCR in SKBR-3 cells (Fig. 2*C*). The results of the cell counting kit-8 (CCK-8) cell viability assay indicate that treatment of cells with various concentrations of trastuzumab (0, 0.05, 0.1, 0.15, 0.2, 0.3, 0.5, 0.75, 10.0 mg/ml) resulted in a significant increase in the inhibitory effect of trastuzumab on SKBR-3TR cell viability. Furthermore, the oe-BANCR group demonstrated a notable reduction in the inhibitory effect of trastuzumab on SKBR-3 cell viability compared to the overexpression negative control (oe-NC) group (Fig. 2*D*). Flow cytometric data indicated that sh-BANCR caused an increase in the apoptosis of SKBR-3TR treated with trastuzumab for 60 h, while oe-BANCR led to a decline in the apoptosis of SKBR-3 cells (Fig. 2*E*).

We repeated the experiments in HCC1954 and HCC1954-TR cells, and the results were consistent with the trends observed in SKBR-3 and SKBR-3TR cells (Fig. S1). The above results confirm that oe-BANCR can enhance the resistance of BC cells to trastuzumab.

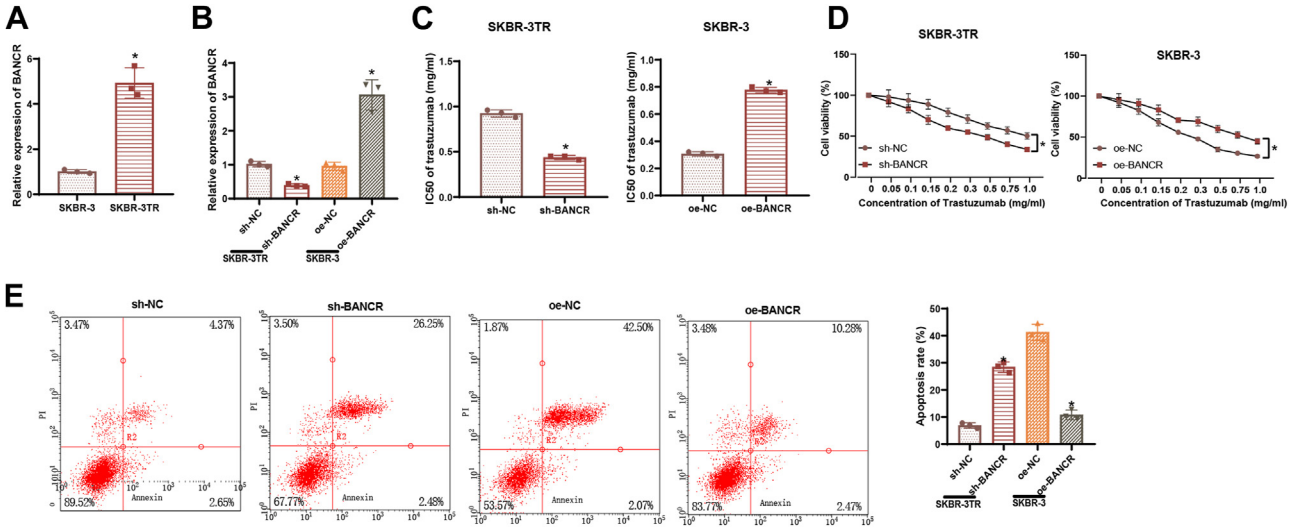

Figure 2. BANCR facilitates the resistance of BC cells to trastuzumab. *A,* BANCR expression in SKBR-3TR and SKBR-3 cells determined by qRT-PCR. *B,* BANCR expression in SKBR-3TR transduced with lentivirus harboring sh-BANCR and SKBR-3 cells harboring oe-BANCR determined by qRT-PCR. *C,* IC_{50} value of trastuzumab in SKBR-3TR treated with sh-BANCR and SKBR-3 cells treated with oe-BANCR determined by CCK-8. *D,* viability of SKBR-3TR treated with sh-BANCR and of SKBR-3 cells treated with oe-BANCR determined by CCK-8. *E,* apoptosis rate of SKBR-3TR treated with sh-BANCR and of SKBR-3 cells treated with oe-BANCR determined by flow cytometry. The apoptotic rate is calculated by summing Q2 (late apoptotic cells) and Q3 (early apoptotic cells). *$p < 0.05$ *versus* sh-NC or oe-NC. Cell experiments were repeated three times. BANCR, BRAF-activated nonprotein coding RNA; BC, breast cancer; Oe-BANCR, overexpression of BANCR.

BC cell–derived EV-mediated transfer of BANCR is involved in the regulation of BC trastuzumab resistance

Then, we sought to explore the mechanism of BANCR in the trastuzumab resistance. RNA-FISH results showed that BANCR was mainly located in the cytoplasm (Fig. 3*A*), which was further demonstrated by qRT-PCR (Fig. 3*B*). In addition, the expression of extracellular BANCR showed no changes in the cell medium added with RNase A, alone while further addition of Triton X-100 decreased the expression of extracellular BANCR (Fig. 3*C*). The above results suggest that the extracellular BANCR is not directly released and may be transferred by membrane wrapping.

To confirm this conjecture, EVs were isolated from the medium of SKBR-3 and SKBR-3TR. The size of the isolated EVs mainly ranged from 75 to 150 nm, and the EVs from the two cells showed similar morphology, size, and number (Fig. 3*D* and *E*). Western blot data found that both TSG-101 and CD81 were expressed in the EVs, not in the cell extracts (Fig. 3*F*), demonstrating the successful separation of EVs. In addition, the expression of BANCR in EVs was not significantly different from that in the cell culture medium, but it almost disappeared after the removal of the EVs from the culture medium (Fig. 3*G*). This result shows that EVs are the main carrier of extracellular BANCR. Meanwhile, the expression of BANCR was higher in SKBR-3TR–derived EVs (SKBR-3TR-EVs) than in SKBR-3 cell–derived EVs (SKBR-3-EVs) (Fig. 3*H*).

Overall, extracellular BANCR is transferred through EVs, and resistant cell–derived EVs carry higher expression of BANCR. BANCR is involved in the regulation of BC resistance through tumor cell–derived EV transfer.

BC cell–derived EV-mediated transfer BANCR increases trastuzumab resistance of BC cells

Based on the aforementioned results, we aimed to explore whether BANCR promotes trastuzumab resistance of BC cells *via* EV transfer. We first isolated EVs from SKBR-3TR, labeled them with PKH26 and then cocultured them with SKBR-3 cells for 48 h. Immunofluorescence data showed strong red signals in SKBR-3 cells (Fig. 4*A*). qRT-PCR data exhibited that BANCR expression was elevated in SKBR-3 cells cocultured with SKBR-3TR-EVs, but it was reduced in the presence of (SKBR-3TR + sh-BANCR) EVs (Fig. 4*B*). The above results prove that BANCR carried by EVs is successfully transferred into the SKBR-3 cells.

Compared to the PBS group, the IC_{50} value of trastuzumab in SKBR-3 cells was significantly higher in the SKBR-3TR EVs group, while cell viability inhibition was markedly lower. Conversely, compared to the SKBR-3TR EVs group, the IC_{50} value of trastuzumab was significantly reduced, and cell viability inhibition was enhanced in the (SKBR-3TR + sh-BANCR) EVs group (Fig. 4*C* and *D*).

To determine whether EVs play a key role in this process, SKBR-3TR cells were treated with the sphingomyelinase inhibitor GW4869 to reduce EV production. Nanoparticle tracking analysis confirmed a significant reduction in EVs derived from SKBR-3TR cells (Fig. 4*E*). CCK-8 assay results showed that compared to the SKBR-3TR EVs group, the IC_{50} value of trastuzumab was significantly reduced, and cell viability inhibition was further enhanced in the (SKBR-3TR + GW4869) EVs group (Fig. 4*F* and *G*).

Under 0.2 mg/ml trastuzumab treatment, flow cytometry revealed reduced apoptosis in the SKBR-3TR EVs group compared to the PBS group. However, apoptosis significantly

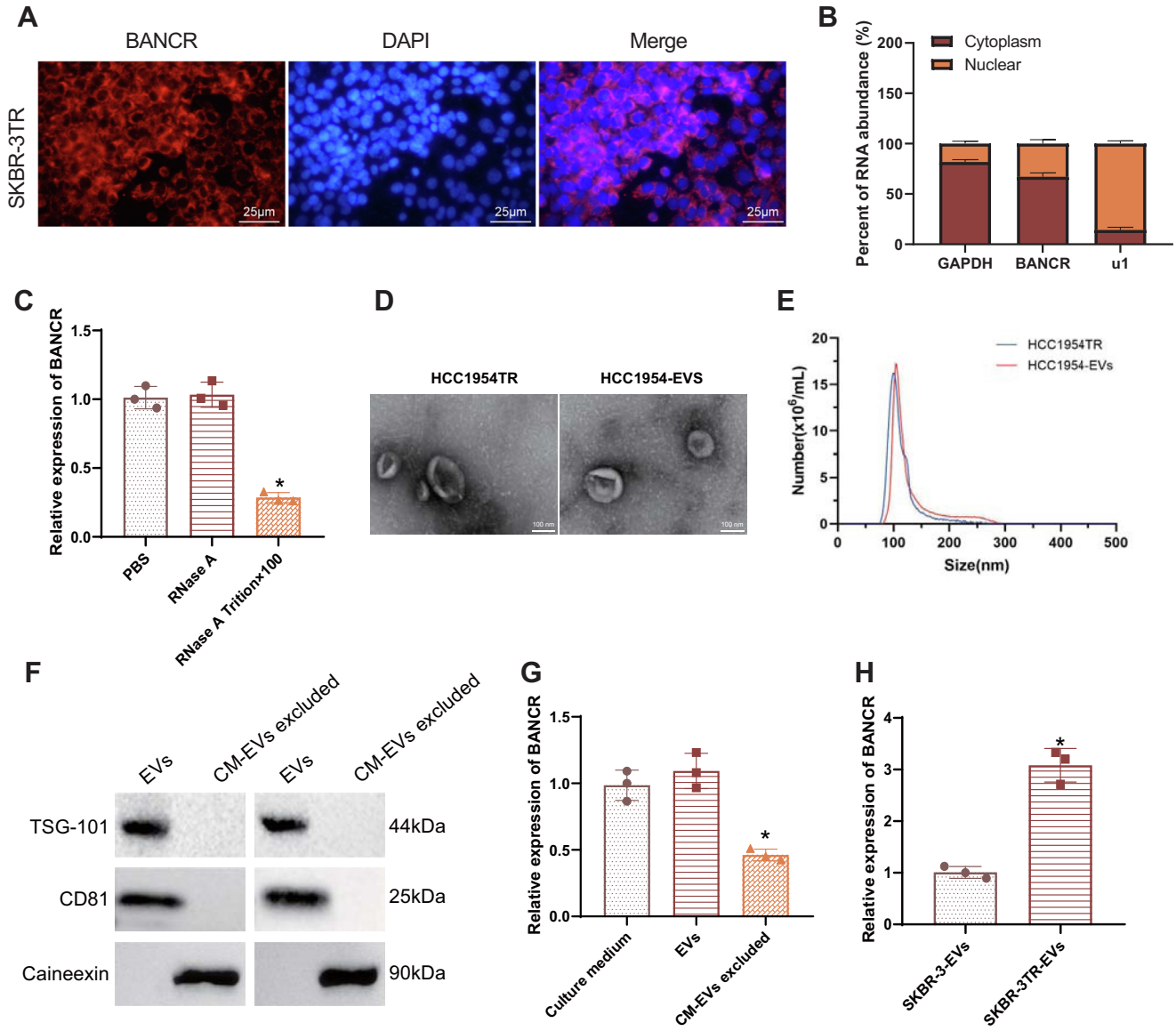

Figure 3. Transfer BANCR *via* BC cell–derived EVs regulates BC trastuzumab resistance. *A,* subcellular localization of BANCR determined by FISH. *Red* indicates BANCR, and *blue* indicates DAPI. *B,* BANCR expression in the nucleus and cytoplasm measured by qRT-PCR. *C,* extracellular BANCR expression in cell medium added with RNase A or combined with Triton X-100 measured by qRT-PCR (*$p < 0.05$ *versus* RNase A). *D,* SKBR-3TR-EVs and SKBR-3-EVs observed under a TEM. *E,* size distribution of SKBR-3TR-EVs and SKBR-3-EVs measured by NTA. *F,* Western blot of EV marker proteins in the SKBR-3TR-EVs and SKBR-3-EVs and cell extracts. *G,* the expression of BANCR in cell culture medium, EVs, and EV-free medium measured by qRT-PCR (*$p < 0.05$ *versus* culture medium). H, The expression of BANCR in SKBR-3TR-EVs and SKBR-3-EVs measured by qRT-PCR (*$p < 0.05$ *verss* SKBR-3 EVs). All data are presented as mean ± SD. Cell experiments were repeated three times. EV, extracellular vesicle; BANCR, BRAF-activated nonprotein c oding RNA; BC, breast cancer; NTA, nanoparticle tracking analysis; TEM, transmission electron microscope.

increased in the (SKBR-3TR + sh-BANCR) EVs and (SKBR-3TR + GW4869) EVs groups compared to the SKBR-3TR EVs group (Fig. 4*H*).

The above results suggest that the promoting effect of BANCR on the trastuzumab resistance of BC cells was achieved through the transfer by BC cell–derived EVs.

BANCR acts as ceRNA to sponge miR-34a-5p to promote trastuzumab resistance of BC cells

The RNA22 website predicted binding sites between BANCR and the miR-34a-5p sequence (Fig. 5*A*). Dual luciferase reporter assay data showed that the luciferase activity of WT was decreased following transfection with miR-34a-5p mimic but that of BANCR-MUT exhibited no alteration (Fig. 5*B*).

In addition, RNA immunoprecipitation (RIP) data indicated that both BANCR and miR-34a-5p were enriched in the anti-AGO2 immunoprecipitation complex (Fig. 5*C*). Down-regulation of BANCR in SKBR-3TR increased the expression of miR-34a-5p (Fig. 5*D*). These lines of evidence prove that BANCR can inhibit the expression of miR-34a-5p by sponging miR-34a-5p as competing endogenous RNA (ceRNA).

The results of qRT-PCR revealed that miR-34a-5p expression was decreased in response to miR-34a-5p inhibitor (Fig. 5*E*). The CCK-8 assay showed that compared to the

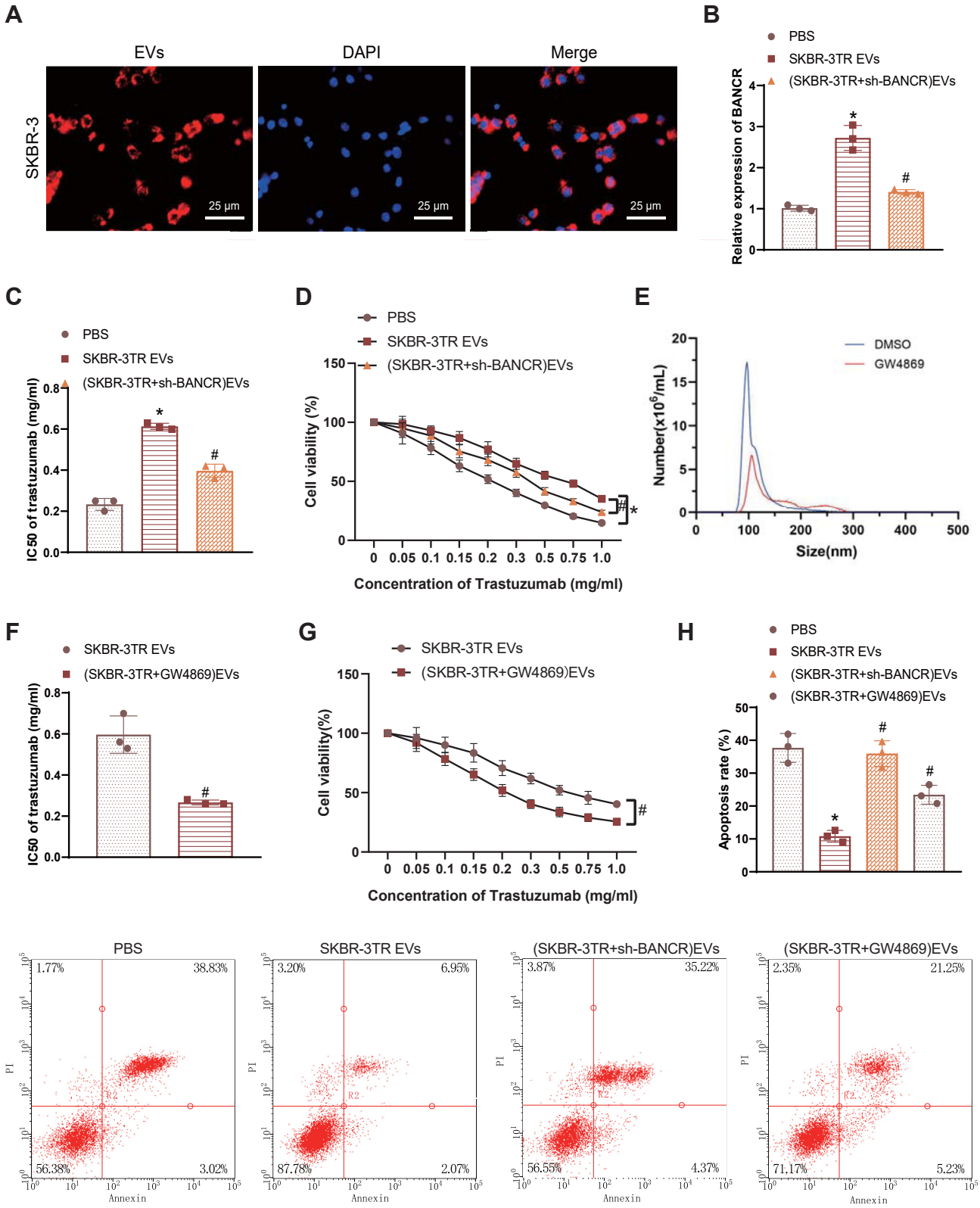

Figure 4. BC cell–derived EVs transfer BANCR to enhance the trastuzumab resistance of BC cells. *A,* uptake of the SKBR-3TR-EVs labeled with PKH26 by SKBR-3 cells. *Red* indicates EVs, and *blue* indicates DAPI. *B,* BANCR expression in SKBR-3 cells cocultured with SKBR-3TR-EVs or (SKBR-3TR + sh-BANCR) EVs determined by qRT-PCR. *C,* IC_{50} value of trastuzumab in SKBR-3 cells cocultured with SKBR-3TR-EVs or (SKBR-3TR + sh-BANCR) EVs determined by CCK-8. *D,* viability of SKBR-3 cells cocultured with SKBR-3TR-EVs or (SKBR-3TR + sh-BANCR) EVs determined by CCK-8. *E,* size distribution and number of SKBR-3TR-EVs upon treatment with GW4869 analyzed by NTA. *F,* IC_{50} value of trastuzumab in SKBR-3 cells cocultured with SKBR-3TR-EVs or (SKBR-3 TR + GW4869) EVs determined by CCK-8. *G,* viability of SKBR-3 cells cocultured with SKBR-3TR-EVs or (SKBR-3TR + GW4869) EVs determined by CCK-8. *H,* apoptosis rate of SKBR-3 cells cocultured with SKBR-3TR-EVs, (SKBR-3TR + sh-BANCR) EVs or (SKBR-3TR + GW4869) EVs determined by flow cytometry. *$p < 0.05$ *versus* PBS, #$p < 0.05$ *versus* SKBR-3TR EVs. All data are presented as mean ± SD. Cell experiments were repeated three times. EV, extracellular vesicle; BANCR, BRAF-activated nonprotein coding RNA; BC, breast cancer; NTA, nanoparticle tracking analysis.

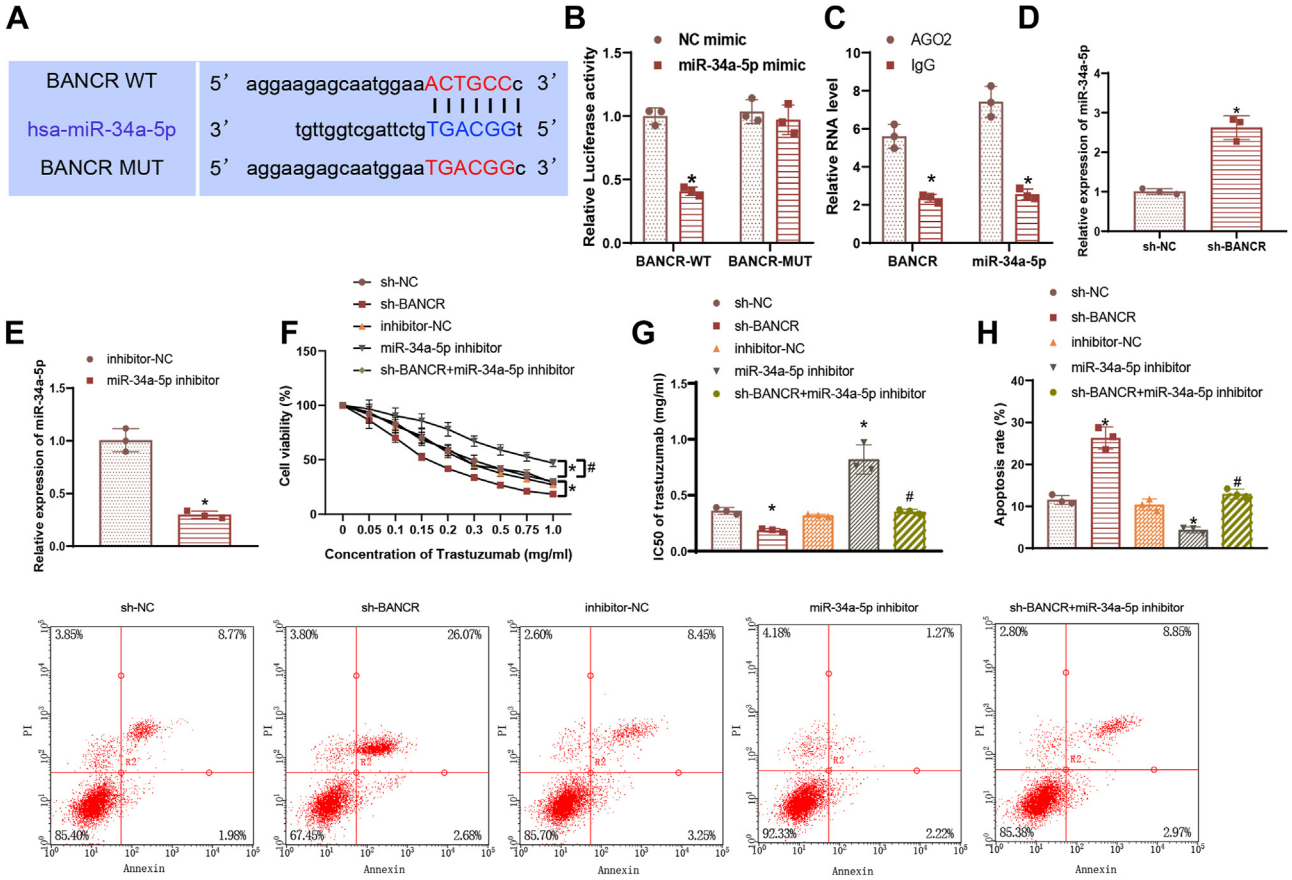

Figure 5. BANCR facilitates trastuzumab resistance of BC cells by acting as ceRNA to sponge miR-34a-5p. *A,* binding sites of BANCR to the miR-34a-5p sequence predicted by RNA22 website. *B,* the binding of BANCR to miR-34a-5p verified by dual luciferase reporter assay (*$p < 0.05$ *versus* mimic-NC). *C,* the binding of BANCR to miR-34a-5p analyzed by RIP assay (*$p < 0.05$ *versus* IgG). *D,* the expression of miR-34a-5p in SKBR-3TR after BANCR downregulation measured by qRT-PCR (*$p < 0.05$ *versus* sh-NC). *E,* miR-34a-5p inhibition efficiency measured by qRT-PCR. SKBR-3TR were treated with sh-BANCR or combined with miR-34a-5p inhibitor (*$p < 0.05$ *versus* inhibitor-NC). *F,* IC_{50} value of trastuzumab in SKBR-3TR determined by CCK-8. *G,* viability of SKBR-3TR determined by CCK-8. *H,* apoptosis rate of SKBR-3TR determined by flow cytometry. In panel *F–H*, *$p < 0.05$ *versus* sh-NC or inhibitor-NC, #$p < 0.05$ *versus* sh-BANCR. Cell experiments were repeated three times. BANCR, BRAF-activated nonprotein coding RNA; BC, breast cancer.

sh-NC group, the sh-BANCR group had a lower IC_{50} value of trastuzumab and enhanced cell viability inhibition in SKBR-3TR cells. Compared to the inhibitor-NC group, the miR-34a-5p inhibitor group exhibited a higher IC_{50} value and reduced cell viability inhibition. Additionally, the sh-BANCR + miR-34a-5p inhibitor group, compared to the sh-BANCR group, displayed an increased IC_{50} value and decreased cell viability inhibition (Fig. 5*F* and *G*). Moreover, in the absence of BANCR, SKBR-3TR apoptosis was accelerated following treatment with trastuzumab, while a reduction was found following further miR-34a-5p inhibition.

Additionally, miR-34a-5p inhibitor suppressed the apoptosis of 0.2 mg/ml trastuzumab-treated SKBR-3TR (Fig. 5*H*).

Altogether, BANCR can promote trastuzumab resistance of BC cells by acting as ceRNA to sponge miR-34a-5p.

BANCR-mediated miR-34a-5p inhibition activates the HMGA1/Wnt/β-catenin axis and promotes trastuzumab resistance of BC cells

Subsequently, the focus was on probing into the mechanism by which BANCR regulates miR-34a-5p to promote trastuzumab resistance of BC cells. Starbase and miRWalk websites were employed to predict downstream target genes of miR-34a-5p. Differential analysis of the GSE24460 mRNA expression dataset yielded 255 upregulated mRNAs and 223 downregulated mRNAs in the BC-resistant samples. In addition, differential analysis of the GSE89216 dataset yielded 276 mRNAs and 324 downregulated mRNAs in BC-resistant samples (Fig. 6, *A–D*). The predicted downstream targets of miR-34a-5p were intersected with the upregulated mRNAs in BC-resistant samples, and three genes of HMGA1, TM4SF1, and ARHGAP29 were obtained (Fig. 6*E*). Analysis of the GSE24460 and GSE89216 datasets showed significantly higher expression of HMGA1, TM4SF1, and ARHGAP29 in drug-resistant BC cells than in drug-sensitive BC cells (Figs. 6, *F* and *G*, S2).

StarBase predicted miR-34a-5p binding sites in the HMGA1 sequence, which was further demonstrated by a dual luciferase reporter experiment (Fig. 6, *H* and *I*). BANCR and HMGA1 were found to be positively correlated in BC samples (Fig. 6*J*). qRT-PCR results showed that HMGA1 expression was promoted in the presence of oe-HMGA1 (Fig. 6*K*).

The CCK-8 assay showed that compared to the mimic-NC group, the miR-34a-5p mimic group significantly reduced

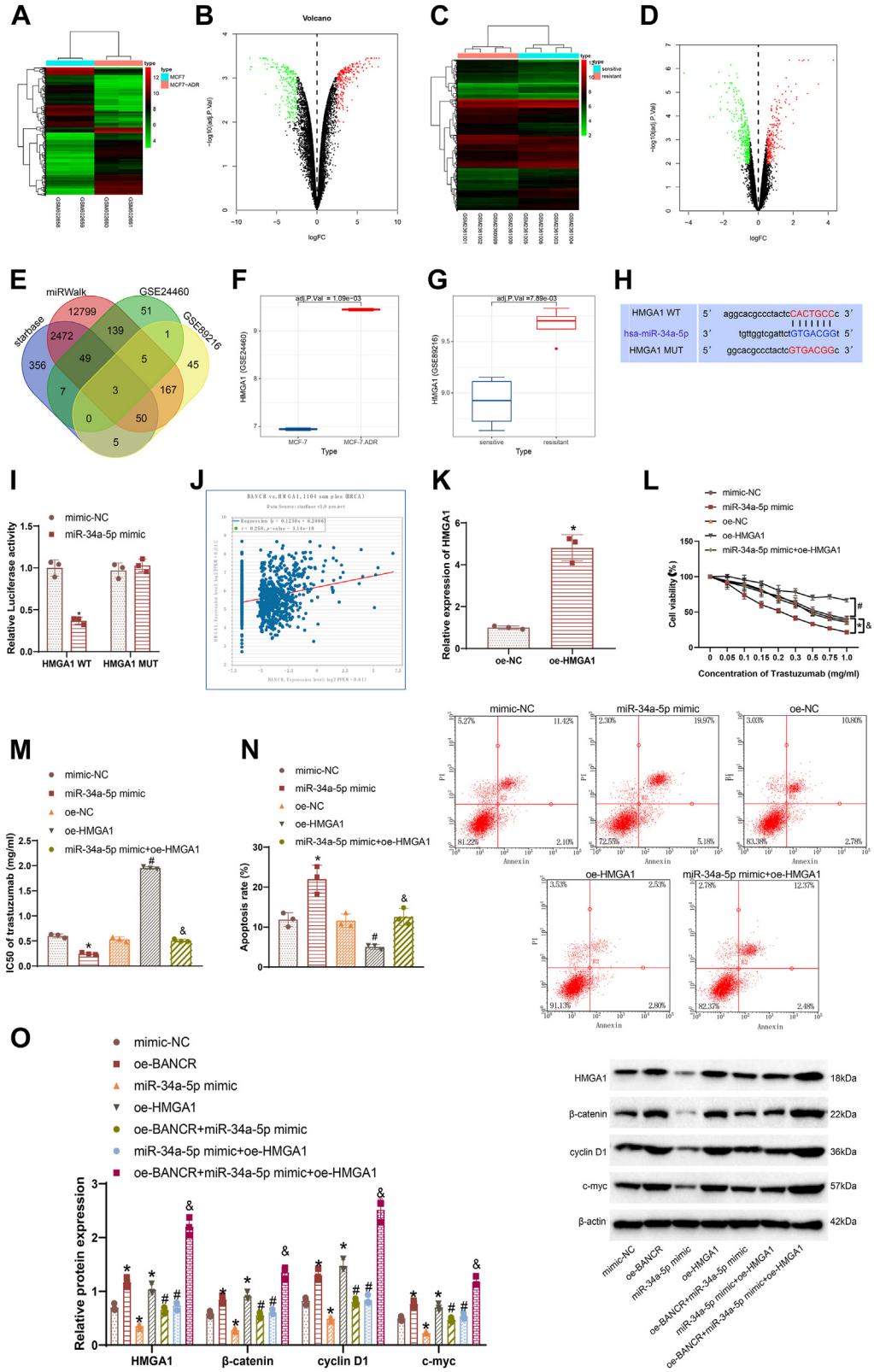

Figure 6. BANCR activates the HMGA1/Wnt/β-catenin axis by competitively binding to miR-34a-5p, thereby inducing trastuzumab resistance of BC cells. *A*, a heat map showing the differentially expressed mRNAs in BC-resistant (n = 2) and BC-sensitive cell line samples (n = 2) in the GSE24460 dataset. *B*, a volcano map showing the differentially expressed mRNAs in BC-resistant (n = 2) and BC-sensitive cell line samples (n = 2) in the GSE24460 dataset. *Red* indicates upregulated mRNAs, and *green* indicates downregulated mRNAs. *C*, a heat map showing the differentially expressed mRNAs in BC-resistant (n = 4) and BC-sensitive cell line samples (n = 4) in the GSE89216 dataset. *D*, a volcano map showing the differentially expressed mRNAs in BC-resistant (n = 4) and BC-sensitive cell line samples (n = 4) in the GSE89216 dataset. *Red* indicates upregulated mRNAs, and *green* indicates downregulated mRNAs. *E*, Venn diagram of the downstream targets of miR-34a-5p and the upregulated mRNAs in BC-resistant samples. The *blue circle* represents the prediction results of starBase website, the *red circle* indicates prediction results of miRWalk website, and the *green circle* indicates the highly expressed mRNAs in BC-resistant

trastuzumab's IC_{50} value and enhanced cell viability inhibition in SKBR-3TR cells. Compared to the oe-NC group, the oe-HMGA1 group significantly increased the IC_{50} value and reduced cell viability inhibition. Additionally, compared to the miR-34a-5p mimic group, the miR-34a-5p mimic + oe-HMGA1 group significantly raised the IC_{50} value and decreased cell viability inhibition (Fig. 6, *L* and *M*).

As depicted in Figure 6*N*, apoptosis of trastuzumab-treated SKBR-3TR was enhanced following miR-34a-5p mimic transfection, while a reduction was found following oe-HMGA1 transduction.

Western blot results showed that oe-BANCR or oe-HMGA1 transduction elevated the protein expression of HMGA1, β-catenin, cyclin D1, and c-myc, while this elevation was reversed following overexpression of miR-34a-5p. Besides, oe-BANCR + miR-34a-5p mimic + oe-HMGA1 increased the protein expression of β-catenin, cyclin D1, and c-myc (Fig. 6*O*).

The aforementioned data support that BANCR can activate the HMGA1/Wnt/β-catenin axis by competitively inhibiting miR-34a-5p, thereby promoting trastuzumab resistance of BC cells.

CBP mediates the acetylation of H3K27 and activates BANCR

Bioinformatics analysis revealed higher H3K27ac enrichment in the BANCR promoter region (Fig. 7*A*). Chromatin immunoprecipitation (ChIP) further showed higher enrichment of H3K27ac in the BANCR promoter region in SKBR-3TR than in SKBR-3 cells (Fig. 7*B*). C646 is a competitive and selective histone acetyltransferase inhibitor targeting p300, suppressing acetylation of histones/non-histones and chromatin transcription dependent on histone acetyltransferases (17, 18). In addition, qRT-PCR found that the expression of BANCR was reduced in C646-treated SKBR-3TR (Fig. 7*C*).

ChIP assay confirmed the CREB-binding protein (CBP) enrichment in the BANCR promoter (Fig. 7*D*). CBP gene was knocked down in SKBR-3TR and the knockdown efficiency was measured by Western blot (Fig. 7*E*). ChIP assay found that the H3K27 acetylation level in the BANCR promoter region was also decreased after CBP inhibition (Fig. 7*F*). In addition, the expression of BANCR was diminished with CBP knockdown (Fig. 7*G*).

The above results indicate that CBP-mediated acetylation of H3K27 can activate BANCR and promote BANCR expression.

Inhibition of BANCR reverses tumorigenicity and trastuzumab resistance of BC cells in nude mice

Finally, we intended to explore the effect of BANCR on trastuzumab resistance of BC cells *in vivo*. SKBR-3TR were transduced with lentivirus carrying sh-NC and sh-BANCR, and cells that stably downregulated BANCR were screened by qRT-PCR (Fig. 8*A*). After injecting the cell suspension subcutaneously into nude mice, we initially observed that the treatment with sh-BANCR did not directly affect tumor growth *in vivo* (Fig. S3). After 25 days, the mice were euthanized, and xenograft tumors were removed and weighed. Results showed that trastuzumab treatment significantly reduced tumor volume and weight in the sh-BANCR group compared to the sh-NC group (Fig. 8, *B–D*).

Immunohistochemical analysis revealed that HMGA1, β-catenin, cyclin D1, and c-myc expression levels were markedly lower in the sh-BANCR group under trastuzumab treatment (Fig. 8*E*). These findings suggest that BANCR inhibition reverses tumorigenic capacity and trastuzumab resistance *in vivo*.

Discussion

This study demonstrated that BANCR encapsulated in BC cell–derived EVs may confer trastuzumab resistance of BC cells, which was associated with the competitive binding to miR-34a-5p and activation of the HMGA1/Wnt/β-catenin pathway.

Increasing numbers of studies have shown that lncRNAs promote drug resistance in BC (19–21). This study is the first case to report that BANCR facilitated the resistance of BC cells to trastuzumab. BANCR knockdown increases the sensitivity of hepatocellular carcinoma cells to sorafenib (22). Furthermore, recent work has highlighted that BANCR overexpression promotes the resistance of gastric cancer cells to cisplatin *in vitro* (23). A previous study has identified that BANCR is overexpressed in BC cell lines and tissues, and its ectopic expression promotes BC progression, evidenced by increased tumor size and lymph node metastasis *in vivo*, and triggers migration and invasion of BC cells in MDA-MB-468 cells (24). These data suggest the possible promoting role of BANCR in the resistance of BC cells to trastuzumab.

Subsequent results of this study revealed that the role of BANCR in increasing the trastuzumab resistance of BC cells was associated with the transfer by BC cell–derived EVs. BANCR was enriched in the BC cell–derived EVs and can be transmitted to the BC-sensitive cells, thus inducing trastuzumab resistance. Indeed, tumor-released EV lncRNAs are capable of enhancing the chemoresistance of tumor cells, whereby lncRNAs wrapped in tumor cell–derived EVs can be transferred to nonresistant cells and thus disseminate drug resistance (25–27).

samples in the GSE24460 dataset, while the *yellow circle* indicates the highly expressed mRNAs in BC-resistant samples in the GSE89216 dataset. *F,* HMGA1 expression in BC-resistant (n = 2) and BC-sensitive cell line samples (n = 2) in the GSE24460 dataset. *G,* HMGA1 expression in BC-resistant (n = 4) and BC-sensitive cell line samples (n = 4) in the GSE89216 dataset. *H,* binding sites of miR-34a-5p in the sequence of HMGA1 predicted by starBase website. *I,* binding of miR-34a-5p to HMGA1 verified by dual-luciferase reporter experiment. *J,* correlation of BANCR expression and HMGA1 expression in BC samples (n = 1104) analyzed by starBase website. *K,* overexpression efficiency of HMGA1 determined by qRT-PCR (*$p < 0.05$). SKBR-3TR were treated with miR-34a-5p mimic, oe-HMGA1 alone or in combination. *L,* viability of SKBR-3TR determined by CCK-8. *M,* IC_{50} value of trastuzumab in SKBR-3TR determined by CCK-8. *N,* apoptosis rate of SKBR-3TR determined by flow cytometry. *O,* Western blot of the Wnt/β-catenin–related proteins. In panel *L–O*, *$p < 0.05$ *versus* mimic-NC, #$p < 0.05$ *versus* Oe-BANCR, miR-34a-5p mimic, or oe-HMGA1, and $p < 0.05$ *versus* oe-BANCR + oe-miR-34a-5p or oe-miR-34a-5p + oe-HMGA1. Cell experiments were repeated three times. BANCR, BRAF-activated nonprotein coding RNA; BC, breast cancer; HMGA1, high-mobility group A1; Oe-BANCR, overexpression of BANCR.

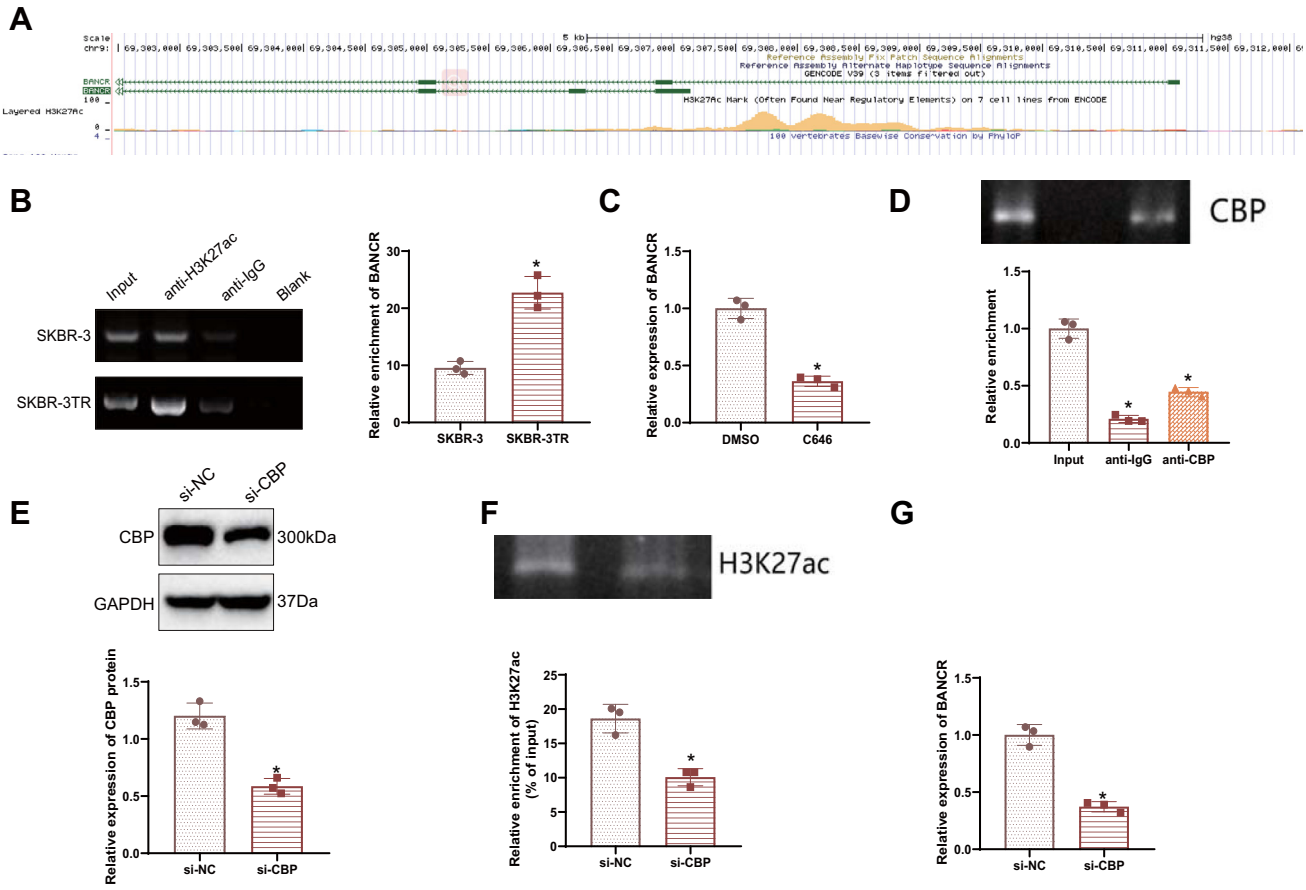

Figure 7. CBP elevates BANCR expression by mediating acetylation of H3K27. *A,* H3K27ac enrichment in the BANCR promoter region through the UCSC website. *B,* H3K27ac enrichment in the BANCR promoter region analyzed by ChIP. *C,* BANCR expression in SKBR-3TR treated with C646 for 48 h determined by qRT-PCR. *D,* CBP enrichment in the BANCR promoter region in SKBR-3TR analyzed by ChIP. *E,* CBP knockdown efficiency measured by Western blot. *F,* H3K27ac enrichment in the BANCR promoter region in SKBR-3TR after CBP knockdown. *G,* BANCR expression in SKBR-3TR after CBP knockdown measured by qRT-PCR. *$p < 0.05$. Cell experiments were repeated three times. BANCR, BRAF-activated nonprotein coding RNA; ChIP, chromatin immunoprecipitation.

BANCR has been reported to act as ceRNA to sponge miRNAs, such as miR-338-3p, miR-204, and miR-195-5p, and thereby decrease their expression (28–30). The current study first demonstrated that BANCR acted as a ceRNA to sponge miR-34a-5p to downregulate its expression, thereby inducing the trastuzumab resistance of BC cells. In line with this finding, previous literature has suggested that miR-34a expression is significantly downregulated in the adriamycin-resistant MCF-7 cell lines compared with its parental cell lines; ectopic expression of miR-34a has been reported to sensitize MCF-7 BC cells to adriamycin *via* targeting Notch1 (31). Emerging evidence demonstrates that miRNAs can interact with the 3′UTR of specific target mRNAs and consequently suppress their expression (32, 33). In this study, the bioinformatics website, together with dual luciferase reporter assay, demonstrated that miR-34a-5p could bind to the 3′UTR of HMGA1 mRNA and consequently negatively regulate its expression. This indicates the first evidence for the posttranscriptional regulation of HMGA1 by miR-34a-5p in BC cells and may have significance in the regulation of BC progression.

Knockdown of HMGA1 overcomes the resistance of ovarian cancer cells to chemotherapeutic agents, whereas its overexpression increases cell resistance (13). In addition, HMGA1 can promote the chemoresistance of glioma cells by regulating the expression of MYH9 through c-Jun–mediated transcription (34). Here, we show for the first time that HMGA1 expression has a substantial value as a biomarker of response to chemotherapy in BC. In addition, the contribution of HMGA1 to the activation of the Wnt/β-catenin pathway has been extensively reported (35, 36). Meanwhile, the trastuzumab resistance in SKBR3/100-8 and BT474/100-2 was accompanied with activation of the Wnt/β-catenin pathway (37). In lieu of the above-mentioned findings and evidence, we can conclude that BANCR may activate the HMGA1/Wnt/β-catenin axis by competitively binding to miR-34a-5p, thereby promoting trastuzumab resistance of BC cells.

This study also uncovered the upstream mechanism underlying the upregulation of BANCR in BC, which was due to the CBP mediation on the acetylation of H3K27. It has been found that abnormal expression of lncRNAs is usually caused by acetylation-mediated transcriptional activation (38). CBP plays a key role in chromatin acetylation (39, 40).

While this study consistently demonstrated the role of BANCR in two HER2-positive, trastuzumab-resistant breast cancer cell models (SKBR-3TR and HCC1954TR) through functional assays such as IC_{50} determination, cell viability, and

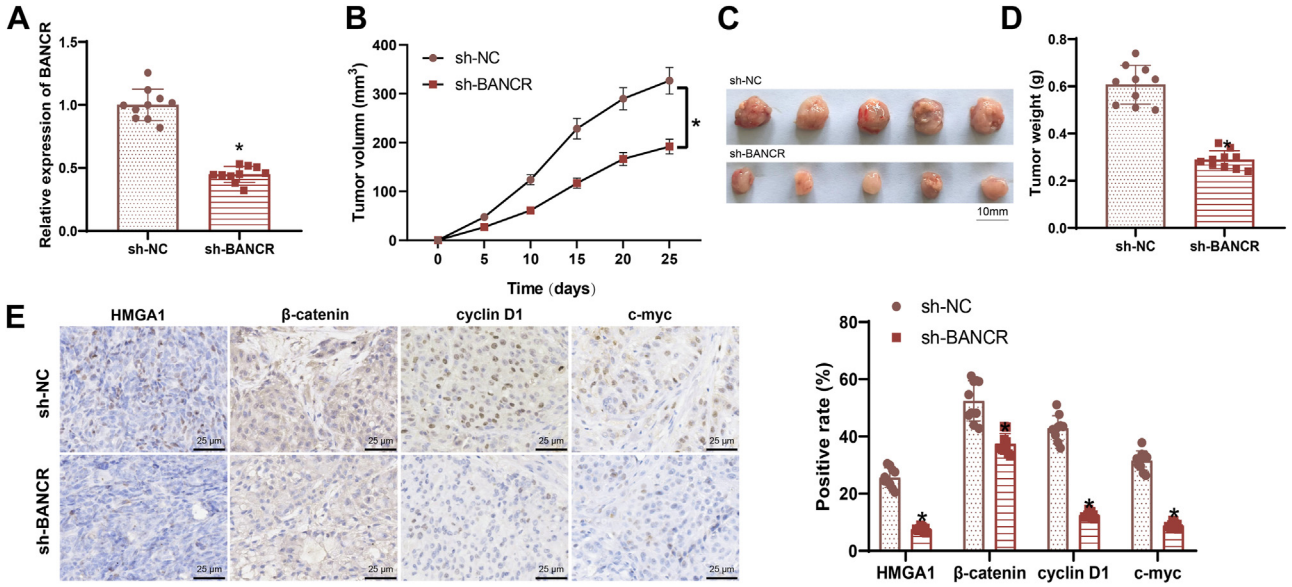

Figure 8. The effect of BANCR on the resistance and metastasis of breast cancer cells to trastuzumab *in vivo*. *A,* qRT-PCR detection of the down-regulation efficiency of BANCR after lentivirus infection; *B,* line graph of tumor volume changes in nude mice from each group after trastuzumab treatment; *C,* images of tumors from nude mice in each group after trastuzumab treatment; *D,* comparison of tumor weights in nude mice from each group after trastuzumab treatment; *E,* immunohistochemical detection of relevant protein expression in tumor tissues from each group of nude mice after trastuzumab treatment; the horizontal line in the bottom right corner represents 25 μm (* indicates a significant difference between the two groups with $p < 0.05$; n = 10). LncRNA, long noncoding RNA; EV, extracellular vesicle; BANCR, BRAF-activated nonprotein coding RNA; BC, breast cancer.

apoptosis, mechanistic studies were predominantly conducted in SKBR-3TR cells. The omission of detailed mechanistic investigations in HCC1954TR cells, such as miR-34a-5p mimic assays and HMGA1 regulation, was primarily due to resource constraints and time limitations. Furthermore, the extensive mechanistic insights obtained from SKBR-3TR cells were deemed sufficient to elucidate the primary regulatory role of BANCR in trastuzumab resistance. However, this selective focus may limit the generalizability of our findings across other trastuzumab-resistant models. Future research should extend mechanistic studies to HCC1954TR and additional models to validate BANCR's interactions with miR-34a-5p and the HMGA1/Wnt/β-catenin signaling pathway, ensuring broader applicability of the results.

Taken together, the present study highlights the pivotal role of BANCR in trastuzumab resistance. BANCR can be incorporated into the BC cell–derived EVs and transmitted to the BC-sensitive cells. BANCR sponges miR-34a-5p and reduces miR-34a-5p binding to HMGA1, thus upregulating the expression of HMGA1 and activating the Wnt/β-catenin pathway. By this mechanism, the trastuzumab resistance of BC cells is enhanced (Fig. 9). These findings show that BANCR could not only act as a predictor of tumor response to trastuzumab-based chemotherapy but also as a potential to develop new strategies in treating BC.

Experimental procedures

Ethics statement

Animal experiments were approved by the Animal Ethics Committee of the Affiliated Hospital of Guangdong Medical University (SUMC-IRB-2021) and strictly performed according to *the Guide for the Care and Use of Laboratory Animals* published by the US National Institutes of Health.

In silico *prediction*

Trastuzumab-resistant and trastuzumab-sensitive lncRNA expression dataset GSE155478 (3 BC-sensitive samples and 3 BC-resistant samples) was retrieved from the GEO database and subjected to differential analysis using R "limma" package with $|\log FC| > 2$ and $p < 0.01$ as the screening criteria. LncRNA expression dataset GSE115040 of EVs and BC cell lines (3 BC samples and 3 EV samples) was retrieved from the GEO database, followed by differential analysis using R "limma" package with $|\log FC| > 5$ and $p < 0.01$ as the screening criteria. Next, highly expressed lncRNAs in BC-resistant cell lines and significantly enriched lncRNAs in EVs were intersected to screen candidate lncRNAs secreted by EVs that may affect BC resistance. Combined with existing literature, candidate downstream miRNAs of lncRNAs in the regulation of BC resistance were identified. Binding sites between lncRNAs and miRNAs were predicted using the RNA22 website. Downstream target genes of miR-34a-5p were predicted using starBase and miRWalk websites.

BC-resistant and BC-sensitive mRNA expression datasets GSE24460 (2 BC-sensitive samples and 2 BC-resistant samples) and GSE89216 (4 BC-sensitive samples and 4 BC-resistant samples) were retrieved from the GEO database. Differential analysis of the two datasets was conducted using the R "limma" package with $|\log FC| > 2.5$ and $p < 0.01$, and $|\log FC| > 0.5$ and $p < 0.01$, as the threshold, respectively.

The significantly highly expressed mRNAs in BC-resistant samples from GEO database were intersected with the

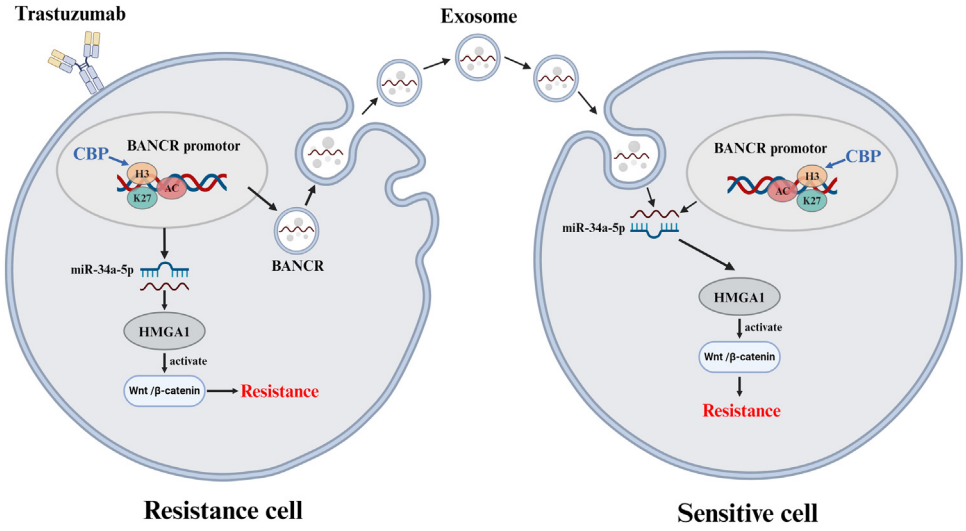

Figure 9. Molecular mechanism graph of BANCR in trastuzumab resistance of BC cells. BC cell–derived EVs transfer BANCR into BC cells, where BANCR competitively binds to miR-34a-5p and activates the HMGA1/Wnt/β-catenin pathway, thus promoting trastuzumab resistance of BC cells. HMGA1, high-mobility group A1; EV, extracellular vesicle; BANCR, BRAF-activated nonprotein coding RNA; BC, breast cancer.

mRNAs predicted by starBase and miRWalk websites to obtain the miRNA downstream regulatory target genes. The GEPIA website was used to predict the expression of target genes in BC samples. Correlation between the expression of lncRNAs and target genes in BC samples was analyzed by the starBase website.

In vitro *cell culture and establishment of drug-resistant cell line*

BC cell line SKBR-3 (CC-Y1462; Shanghai EK-Bioscience Biotechnology Co., Ltd) was cultured in McCoy's 5A medium (16600082) supplemented with 10% fetal bovine serum (10099158) and 1% penicillin-streptomycin (15,240,062) in a 5% CO_2 incubator at 37 °C. The BC cells HCC1954 were purchased from San Bio (catalog number: SNL-542, https://www.sanbio.com.cn). They were cultured in 1640 medium (catalog number: 11875119, purchased from Thermo Fisher Scientific) supplemented with 10% fetal bovine serum and 1% P/S and incubated at 37 °C in a humidified atmosphere containing 5% CO_2.

The SKBR-3 or HCC1954 cells, obtained from Beijing Bio-Fountain Biotechnology Company (catalog number: 1826843-81-5, http://www.bio-fountain.com), were dissolved in PBS for use. Subsequently, 5×10^6 cells were subcutaneously injected into the flanks of nude mice. Once the xenografts reached the size of a soybean, intraperitoneal injections of trastuzumab (3 mg/kg) or PBS were administered every other day for 2 weeks, followed by a 2-week period without drug treatment (completing one cycle). After completion of a treatment cycle, the xenografted BC cells were isolated and reimplanted into new nude mice, and the trastuzumab treatment was continued. BC cells resistant to trastuzumab, known as SKBR-3TR or HCC1954TR, were isolated from the third generation xenografts, with significantly lower levels of HER2 protein in the SKBR-3TR cells than SKBR-3 cells (Fig. S4). The culturing methods for SKBR-3TR or HCC1954TR cells were the same as those for SKBR-3 or HCC1954 cells.

Cell treatment and lentiviral transduction

BC cells were transduced with lentivirus carrying oe-NC, oe-BANCR, sh-NC, sh-BANCR, sh-CBP (Supplementary Table 1), and oe-HMGA1 (Hanheng Biotechnology Co., Ltd, at a virus titer of 1×10^9 TU/ml), transfected with plasmids of mimic-NC, miR-34a-5p mimic, inhibitor-NC and miR-34a-5p inhibitor, or treated with sh-BANCR + miR-34a-5p inhibitor. miR-34a-5p mimic (miR10000255-1-5) and miR-34a-5p inhibitor (miR20000255-1-5) were purchased from Guangzhou RiboBio Co., Ltd. The cells were finally treated with puromycin (60210ES25, Yeasen Company) to screen stable cell lines.

qRT-PCR

Total RNA was extracted from cells using TRIzol reagent (16096020, Thermo Fisher Scientific Inc), the concentration and purity of which were determined using NanoDrop One/OneC spectrophotometer (A260/A280 = 2.0, concentration greater than 5 μg/μl). For mRNA detection, a complementary DNA (cDNA) first-strand synthesis kit (D7168L, Beyotime Biotechnology Co., Ltd) was used to synthesize cDNA. For miRNA detection, miRNA first-strand synthesis (Tailing) Kit (B532451, Sangon Biotech Co., Ltd) was used for cDNA synthesis. qRT-PCR was performed with a RT-qPCR kit (Q511-02, Vazyme Biotech) on a Bio-Rad real-time quantitative PCR instrument CFX96. β-Actin served as the loading control of mRNAs and U6 of miR-34a-5p. Primer sequences designed by Sangon are shown in Supplementary Table 2. $2^{-\Delta\Delta Ct}$ was applied for fold change calculation.

Western blot

Tissues and cells were lysed with radio immunoprecipitation assay lysis buffer with 1 mM PMSF for the total protein extraction, with the concentration determined. Subsequently, the protein was separated using 8 to 12% SDS and electro-

transferred to polyvinylidene fluoride membrane. Afterward, the protein-loaded membrane was blocked with 5% skimmed milk and incubated overnight at 4 °C with rabbit primary antibodies, including β-actin (4970, 1:5000, Cell Signaling Technology [CST]), HMGA1 (12094, 1:1000, CST), CBP (7389, 1:1000, CST), β-catenin (8480, 1:1000, CST), cyclin D1 (55506, 1:1000, CST), C-myc (18583, 1:1000, CST), TSG-101 (ab125011, 1:1000, Abcam), CD81 (ab109201, 1:1000, Abcam), calnexin (ab133615, 1:1000, Abcam), and rabbit anti-HER2 (part number: ab134182, 1:1000, purchased from Abcam). The next day, the membrane was incubated with horseradish peroxidase-labeled goat anti-rabbit IgG (ab6721, 1:5000, Abcam). Enhanced chemiluminescence reagent (1705062, Bio-Rad Inc) was used to visualize the results by the Image Quant (https://www.cytivalifesciences.com/en/us/shop/equipment/imaging-systems/imagequant-las-4000-biomolecular-imager-p-28955837) LAS 4000C Gel Imager, with β-actin used as an internal reference.

CCK-8 assay

Drug toxicity experiment: cell suspension was seeded in a 96-well plate at a density of 5×10^3 cells/well. After 24 h of culture, cells were treated with trastuzumab at various concentrations (0, 0.05, 0.1, 0.15, 0.2, 0.3, 0.5, 0.75, and 1.0 mg/ml diluted in PBS) for 48 h. Next, each well was incubated with 110 μl CCK-8 mixture (100 μl Dulbecco's modified Eagle's medium, 11965092, Thermo Fisher Scientific) and 10 μl CCK-8 reagent (C0037, Beyotime) in a 37 °C incubator for 0.5 to 2 h. A_{450} was measured using a microplate reader, and the IC_{50} value was calculated using SPSS 21.0 statistical software (https://www.ibm.com/support/pages/downloading-ibm-spss-statistics-21).

Cell viability experiment: cell suspension was seeded in a 96-well plate at a density of 5×10^3 cells/well. After 24 h of culture, cells were treated with trastuzumab solution for 0, 12, 24, 36, 48, and 60 h and incubated with 10 cubCCK-8 reagent at the corresponding time point. Next, A_{450} was measured using a microplate reader, and cell viability was calculated using GraphPad Prism 7 software (https://www.graphpad.com/support/prism-7-updates/).

Flow cytometry

Annexin V-FITC/propidium iodide kit (C1062L, Beyotime) was used to determine cell apoptosis. Cells were cultured in an incubator for 48 h, collected in 200 μl buffer, and incubated with 10 μl annexin V-FITC and 5 μl propidium iodide for 15 min at room temperature in the dark. Following treatment with 300 μl buffer, apoptosis was measured using an Attune NxT flow cytometer (Thermo Fisher Scientific). The apoptosis rate is calculated by summing Q2 (late-stage apoptotic cells) and Q3 (early-stage apoptotic cells).

Isolation and identification of EVs

BC cell culture medium was centrifuged at 10,000*g* for 30 min to remove dead cells and cell debris and then at 100,000*g* for 90 min using a Sorvall MTX 150 centrifuge (46963, Thermo Fisher Scientific). The EVs were resuspended in 1 ml of PBS and 25 ml of cold PBS and further ultracentrifuged at 100,000*g* for 70 min to remove the residual medium. Finally, the EVs were resuspended in 100 μl of PBS and stored at −80 °C. All centrifugation steps were performed at 4 °C.

The size distribution of EVs was analyzed by nanoparticle tracking analysis using a NanoSight NS300 instrument (Malvern Instruments), and data analysis was performed using NanoSight NTA3.2 software (https://www.malvernpanalytical.com/en/support/product-support/software/nanosight-nta-software-update-v3-2). In addition, the morphology of EVs was observed and photographed under a transmission electron microscope (GLACIOSTEM, Thermo Fisher Scientific). EV marker proteins TSG-101, CD81, and calnexin were determined by Western blot.

Uptake of EVs by SKBR-3 cells

Isolated EVs were stained using red lipophilic fluorescent dye PKH26 (PKH26PCL, Sigma). The labeled EVs were then incubated with the cultured SKBR-3 cells. After 48 h, the cell nuclei were stained with 4',6-diamidino-2-phenylindole (D9542, Sigma) for 5 min. Fluorescent signals were detected using a laser confocal microscope (FV3000, Olympus) to determine the uptake of EVs by SKBR-3 cells.

RIP assay

RIP kit (RIP-12RXN, Sigma-Aldrich) was applied for this assay. Cells were lysed in RIP lysis buffer, and the cell lysates were incubated with 5 μg anti-AGO2 antibody (1: 100, ab186733, Abcam) and anti-IgG antibody (1: 100, ab200699, Abcam) overnight at 4 °C. Magnetic beads were then added to the cell lysates and incubated at 4 °C for 1 h. Samples were incubated with protease K at 55 °C for 1 h, after which RNA was extracted, purified, and subjected to qRT-PCR to determine the enrichment of BANCR and miR-34a-5p.

Chromatin immunoprecipitation

ChIP was performed using a ChIP kit (P2078, Beyotime). Cells were fixed with 1% paraformaldehyde for 10 min to generate a DNA-protein cross-link, which was halted by glycine. Cell lysates were sonicated to produce 400 to 800 bp chromatin fragments and then immunoprecipitated with rabbit antibodies against IgG (ab172730, 1: 100, Abcam), H3K27ac (ab4729, 1:20, Abcam), and CBP (ab253202, 1: 20, Abcam). Finally, the precipitated BANCR promoter was analyzed by qRT-PCR. BANCR ChIP primer was forward: 5′-TACTTGAGGCAGGCCTGGTA-3′ and reverse: 5′-CTTGTGGGGCACCCTAACTT-3′.

Fluorescent in situ hybridization

Subcellular localization of BANCR was determined using a FISH kit (F32956, Thermo Fisher Scientific). Probe synthesis, labeling, purification, and labeled specimen imaging were performed according to the kit instructions. Fluorescence images were photographed and recorded under a laser confocal scanning microscope (FV3000, Olympus).

Fractionation of nuclear/cytoplasmic RNA

Cytoplasmic and Nuclear RNA Extraction and Purification Kit (21000, Norgen Biotek, Germany) was used for this experiment. A total of 5 t 10^6 cells were resuspended in 0.6 ml resuscitation buffer and incubated for 15 min. Cells were then centrifuged at 400*g* for 15 min, the supernatant was harvested, namely, cytoplasm. The cell precipitate was resuspended in 0.3 ml PBS, 0.3 ml nuclear separation buffer, and 0.3 ml enzyme-free water and incubated on ice for 20 min, with the precipitate obtained, namely, nuclear fragments. RNA expression was determined by qPCR using GAPDH as a cytoplasmic control and U1 snRNA as a nuclear control.

Dual-luciferase reporter assay

BANCR 3′UTR gene fragments (BANCR-3′UTR-WT and BANCR-3′UTR-MUT) with miR-34a-5p binding sites were synthesized and cloned into the pMIR-REPORT vector (AM5795, Thermo Fisher Scientific) containing firefly luciferase reporter gene. After restriction endonuclease cleavage, the target fragment was cloned into the vector using T4 DNA ligase (M0204S, New England BioLabs). HEK293T cells were cotransfected with the 300 ng constructed pMIR-REPORT plasmid, 10 ng pRL-CMV (renilla luciferase gene vector, E2261, Promega), and 50 nM mimic-NC and miR-34a-5p mimic using Lipofectamine 3000 reagent (L3000001, Thermo Fisher Scientific). After 48 h, luciferase activity was detected on a GloMax 20/20 Luminometer (E5311, Promega) using Dual-Luciferase Reporter Assay System Kit (E1910, Promega), with renilla luciferase as an internal reference. All vectors were constructed by Sangon.

Nude mouse xenograft model of BC

In total, 40 4-week-old BALB/c nude mice (Beijing Vital River Laboratory Animal Technology Co., Ltd) were housed individually in the SPF laboratory at 22 to 25 °C and 60 to 65% humidity. The mice were acclimated for 1 week before the experiment. The SKBR-3-TR cell suspension (3×10^6 cells) harboring sh-BANCR or sh-NC was injected subcutaneously into the nude mice (n = 10). When the tumor grew to the size of a soybean, the mice received an intraperitoneal injection of 3 mg/kg trastuzumab every 2 days, lasting 25 days. Tumor diameter was recorded every 5 days using a vernier caliper, and the volume was calculated (length × width)2 × 0.5. Mice were euthanized after 25 days of treatment, and then the xenograft tumor was removed, and weighed.

Immunohistochemistry

Paraffin tumor tissue sections were dewaxed, hydrated, and antigen-retrieved. Next, the sections were blocked with normal goat serum (E510009, Sangon) and immunostained with rabbit antibodies to HMGA1 (12094, 1: 2000, CST), β-catenin (8480, 1: 200, CST), cyclin D1 (55506, 1: 1000, CST), and C-myc (ab32072, 1: 500, Abcam) overnight at 4 °C. Subsequently, the sections were immunostained with secondary antibody goat anti-rabbit IgG (ab6721, 1: 500, Abcam) for 30 min and colored with DAB (P0203, Beyotime). Finally, the sections were stained in hematoxylin, dehydrated, cleared and mounted before observation under an upright microscope (BX63, Olympus). Quantitative analysis was performed using ImageJ software (https://imagej.net/ij/download.html).

Statistical analysis

All data were analyzed using SPSS 21.0 software (IBM Corp) and GraphPad Prism7 software. Measurement data were expressed as mean ± SD. Comparison of data between two groups was conducted using an independent sample *t* test and that of data between multiple groups using one-way ANOVA. Cell viability at different time points was analyzed by two-way ANOVA, while tumor volume at various time points was compared by repeated measures ANOVA. $p < 0.05$ indicates a significant difference.

Data availability

The data underlying this article will be shared on reasonable request to the corresponding author.

Supporting information—This article contains supporting information.

Author contribution—X. S., Y. C., and H. L. writing–review and editing; X. S. and S. L. writing–original draft; X. S. software; X. S. and H. L. methodology; X. S. and H. L. conceptualization; S. L. formal analysis; S. L., Y. Z., and Y. C. data curation; Y. C. visualization; Y. C. validation; H. L. project administration; H. L. funding acquisition; Y. Z. supervision.

Funding and additional information—This study was supported by a Postdoctoral Research Initiation Grant from Shantou University (2021022306).

Conflict of interest—The authors declare that they have no conflicts of interest with the contents of this article.

References

1. Fahad Ullah, M. (2019) Breast cancer: current perspectives on the disease status. *Adv. Exp. Med. Biol.* **1152**, 51–64
2. Maximiano, S., Magalhães, P., Guerreiro, M. P., and Morgado, M. (2016) Trastuzumab in the treatment of breast cancer. *BioDrugs* **30**, 75–86
3. Derakhshani, A., Rezaei, Z., Safarpour, H., Sabri, M., Mir, A., Sanati, M. A., *et al.* (2020) Overcoming trastuzumab resistance in HER2-positive breast cancer using combination therapy. *J. Cell. Physiol* **235**, 3142–3156
4. Watanabe, S., Yonesaka, K., Tanizaki, J., Nonagase, Y., Takegawa, N., Haratani, K., *et al.* (2019) Targeting of the HER2/HER3 signaling axis overcomes ligand-mediated resistance to trastuzumab in HER2-positive breast cancer. *Cancer Med.* **8**, 1258–1268
5. Dong, H., Wang, W., Chen, R., Zhang, Y., Zou, K., Ye, M., *et al.* (2018) Exosome-mediated transfer of lncRNA-SNHG14 promotes trastuzumab chemoresistance in breast cancer [retracted in: Int J Oncol. 2022 Aug;61(2):92. doi: 10.3892/ijo.2022.5382] *Int. J. Oncol.* **53**, 1013–1026
6. Chistiakov, D. A., and Chekhonin, V. P. (2014) Extracellular vesicles shed by glioma cells: pathogenic role and clinical value. *Tumour Biol.* **35**, 8425–8438
7. Hussen, B. M., Azimi, T., Abak, A., Hidayat, H. J., Taheri, M., and Ghafouri-Fard, S. (2021) Role of lncRNA BANCR in human cancers: an updated review. *Front. Cell Dev. Biol.* **9**, 689992

8. Lou, K. X., Li, Z. H., Wang, P., Liu, Z., Chen, Y., Wang, X. L., *et al.* (2018) Long non-coding RNA BANCR indicates poor prognosis for breast cancer and promotes cell proliferation and invasion. *Eur. Rev. Med. Pharmacol. Sci.* **22**, 1358–1365
9. Ma, S., Yang, D., Liu, Y., Wang, Y., Lin, T., Li, Y., *et al.* (2018) LncRNA BANCR promotes tumorigenesis and enhances adriamycin resistance in colorectal cancer. *Aging (Albany NY)* **10**, 2062–2078
10. Kaboli, P. J., Rahmat, A., Ismail, P., and Ling, K. H. (2015) MicroRNA-based therapy and breast cancer: a comprehensive review of novel therapeutic strategies from diagnosis to treatment. *Pharmacol. Res.* **97**, 104–121
11. Zhang, L., Wang, L., Dong, D., Wang, Z., Ji, W., Yu, M., *et al.* (2019) MiR-34b/c-5p and the neurokinin-1 receptor regulate breast cancer cell proliferation and apoptosis. *Cell Prolif* **52**, e12527
12. Li, Z. H., Weng, X., Xiong, Q. Y., Tu, J. H., Xiao, A., Qiu, W., *et al.* (2017) miR-34a expression in human breast cancer is associated with drug resistance. *Oncotarget* **8**, 106270–106282
13. Kim, D. K., Seo, E. J., Choi, E. J., Lee, S. I., Kwon, Y. W., Jang, I. H., *et al.* (2016) Crucial role of HMGA1 in the self-renewal and drug resistance of ovarian cancer stem cells. *Exp. Mol. Med.* **48**, e255
14. Xing, J., Cao, G., and Fu, C. (2014) HMGA1 interacts with β-catenin to positively regulate Wnt/β-catenin signaling in colorectal cancer cells. *Pathol. Oncol. Res.* **20**, 847–851
15. Zhang, W., Zhao, H., Chen, K., and Huang, Y. (2020) Overexpressing of POU2F2 accelerates fracture healing via regulating HMGA1/Wnt/β-catenin signaling pathway. *Biosci. Biotechnol. Biochem.* **84**, 491–499
16. Cheng, S., Huang, Y., Lou, C., He, Y., Zhang, Y., and Zhang, Q. (2019) FSTL1 enhances chemoresistance and maintains stemness in breast cancer cells via integrin β3/Wnt signaling under miR-137 regulation. *Cancer Biol. Ther.* **20**, 328–337
17. Bowers, E. M., Yan, G., Mukherjee, C., Orry, A., Wang, L., Holbert, M. A., *et al.* (2010) Virtual ligand screening of the p300/CBP histone acetyltransferase: identification of a selective small molecule inhibitor. *Chem. Biol.* **17**, 471–482
18. Oike, T., Komachi, M., Ogiwara, H., Amornwichet, N., Saitoh, Y., Torikai, K., *et al.* (2014) C646, a selective small molecule inhibitor of histone acetyltransferase p300, radiosensitizes lung cancer cells by enhancing mitotic catastrophe. *Radiother. Oncol.* **111**, 222–227
19. Yousefi, H., Maheronnaghsh, M., Molaei, F., Mashouri, L., Reza Aref, A., Momeny, M., *et al.* (2020) Long noncoding RNAs and exosomal lncRNAs: classification, and mechanisms in breast cancer metastasis and drug resistance. *Oncogene* **39**, 953–974
20. Zhang, M., Yang, L., Hou, L., and Tang, X. (2021) LncRNA SNHG1 promotes tumor progression and cisplatin resistance through epigenetically silencing miR-381 in breast cancer. *Bioengineered* **12**, 9239–9250
21. Ma, T., Liang, Y., Li, Y., Song, X., Zhang, N., Li, X., *et al.* (2020) LncRNA LINP1 confers tamoxifen resistance and negatively regulated by ER signaling in breast cancer. *Cell Signal* **68**, 109536
22. Zhou, M., Zhang, G., Hu, J., Zhu, Y., Lan, H., Shen, X., *et al.* (2021) Rutin attenuates sorafenib-induced chemoresistance and autophagy in hepatocellular carcinoma by regulating BANCR/miRNA-590-5P/OLR1 Axis. *Int. J. Biol. Sci.* **17**, 3595–3607
23. Miao, X., Liu, Y., Fan, Y., Wang, G., and Zhu, H. (2021) LncRNA BANCR attenuates the killing capacity of cisplatin on gastric cancer cell through the ERK1/2 pathway. *Cancer Manag. Res.* **13**, 287–296
24. Jiang, J., Shi, S. H., Li, X. J., Sun, L., Ge, Q. D., Li, C., *et al.* (2018) Long non-coding RNA BRAF-regulated lncRNA 1 promotes lymph node invasion, metastasis and proliferation, and predicts poor prognosis in breast cancer. *Oncol. Lett.* **15**, 9543–9552
25. Lei, Y., Guo, W., Chen, B., Chen, L., Gong, J., and Li, W. (2018) Tumor-released lncRNA H19 promotes gefitinib resistance via packaging into exosomes in non-small cell lung cancer. *Oncol. Rep.* **40**, 3438–3446
26. Xu, C. G., Yang, M. F., Ren, Y. Q., Wu, C. H., and Wang, L. Q. (2016) Exosomes mediated transfer of lncRNA UCA1 results in increased tamoxifen resistance in breast cancer cells. *Eur. Rev. Med. Pharmacol. Sci.* **20**, 4362–4368
27. Zhang, W., Cai, X., Yu, J., Lu, X., Qian, Q., and Qian, W. (2018) Exosome-mediated transfer of lncRNA RP11-838N2.4 promotes erlotinib resistance in non-small cell lung cancer. *Int. J. Oncol.* **53**, 527–538 [retracted in: Int J Oncol. 2023 Jan;62(1):10. doi: 10.3892/ijo.2022.5458]
28. Song, W., Wang, K., Yang, X., Dai, W., and Fan, Z. (2020) Long non-coding RNA BANCR mediates esophageal squamous cell carcinoma progression by regulating the IGF1R/Raf/MEK/ERK pathway via miR-338-3p. *Int. J. Mol. Med.* **46**, 1377–1388
29. Cai, B., Zheng, Y., Ma, S., Xing, Q., Wang, X., Yang, B., *et al.* (2017) BANCR contributes to the growth and invasion of melanoma by functioning as a competing endogenous RNA to upregulate Notch2 expression by sponging miR-204. *Int. J. Oncol.* **51**, 1941–1951
30. Wu, X., Xia, T., Cao, M., Zhang, P., Shi, G., Chen, L., *et al.* (2019) LncRNA BANCR promotes pancreatic cancer tumorigenesis via modulating MiR-195-5p/wnt/β-catenin signaling pathway. *Technol. Cancer Res. Treat* **18**, 1533033819887962
31. Li, X. J., Ji, M. H., Zhong, S. L., Zha, Q. B., Xu, J. J., Zhao, J. H., *et al.* (2012) MicroRNA-34a modulates chemosensitivity of breast cancer cells to adriamycin by targeting Notch1. *Arch. Med. Res.* **43**, 514–521
32. Ali, S. Z., Langden, S. S. S., Munkhzul, C., Lee, M., and Song, S. J. (2020) Regulatory mechanism of MicroRNA expression in cancer. *Int. J. Mol. Sci.* **21**, 1723
33. Chan, S. H., and Wang, L. H. (2015) Regulation of cancer metastasis by microRNAs. *J. Biomed. Sci.* **22**, 9
34. Que, T., Zheng, H., Zeng, Y., Liu, X., Qi, G., La, Q., *et al.* (2021) HMGA1 stimulates MYH9-dependent ubiquitination of GSK-3β via PI3K/Akt/c-Jun signaling to promote malignant progression and chemoresistance in gliomas [published correction appears in Cell Death Dis. 2022 Feb 21;13(2):164. doi: 10.1038/s41419-022-04547-9] *Cell Death Dis.* **12**, 1147
35. Xian, L., Georgess, D., Huso, T., Cope, L., Belton, A., Chang, Y. T., *et al.* (2017) HMGA1 amplifies Wnt signalling and expands the intestinal stem cell compartment and Paneth cell niche. *Nat. Commun.* **8**, 15008
36. Ren, J., Yang, M., Xu, F., and Chen, J. (2019) microRNA-758 inhibits the malignant phenotype of osteosarcoma cells by directly targeting HMGA1 and deactivating the Wnt/β-catenin pathway. *Am. J. Cancer Res.* **9**, 36–52
37. Wu, Y., Ginther, C., Kim, J., Mosher, N., Chung, S., Slamon, D., *et al.* (2012) Expression of Wnt3 activates Wnt/β-catenin pathway and promotes EMT-like phenotype in trastuzumab-resistant HER2-overexpressing breast cancer cells. *Mol. Cancer Res.* **10**, 1597–1606
38. Jain, A. K., Xi, Y., McCarthy, R., Allton, K., Akdemir, K. C., Patel, L. R., *et al.* (2016) LncPRESS1 is a p53-regulated LncRNA that safeguards pluripotency by disrupting SIRT6-mediated de-acetylation of histone H3K56. *Mol. Cell* **64**, 967–981
39. Hogg, S. J., Motorna, O., Cluse, L. A., Johanson, T. M., Coughlan, H. D., Raviram, R., *et al.* (2021) Targeting histone acetylation dynamics and oncogenic transcription by catalytic P300/CBP inhibition. *Mol. Cell* **81**, 2183–2200.e13
40. Li, S., Wu, H., Huang, X., Jian, Y., Kong, L., Xu, H., *et al.* (2021) BOP1 confers chemoresistance of triple-negative breast cancer by promoting CBP-mediated β-catenin acetylation. *J. Pathol.* **254**, 265–278